Electronic Supplementary Material (ESI) for Nanoscale.

Supporting Information

High performance, visible to mid-infrared photodetector based on graphene nanoribbons passivated by HfO_2

Xuechao Yu,[a,†] Zhaogang Dong,[b,†] Yanping Liu,[a,†] Tao Liu,[a] Jin Tao,[a] Yongquan Zeng,[a] Joel K. W. Yang[c,b] and Qi Jie Wang[a,d,*]

[a]Center for OptoElectronics and Biophotonics, School of Electrical and Electronic Engineering, Nanyang Technological University, 639798, Singapore.

[b]Institute of Materials Research and Engineering, Agency for Science, Technology and Research (A*STAR), 2 Fusionopolis Way, #08-03 Innovis, 138634, Singapore.

[c]Singapore University of Technology and Design, 8 Somapah Road, 487372, Singapore

[d]Center for Disruptive Photonics Technologies, Nanyang Technological University, 21 Nanyang Link, 637371, Singapore.

†Equal contribution.

*Corresponding email: qjwang@ntu.edu.sg

1. Methods.

Sample Preparation: Highly-ordered pyrolytic graphite (HOPG) was purchased from SPI supplies. Monolayer graphene was fabricated by a 3M tape-based mechanical exfoliation on SiO_2/Si wafer with 285 nm thermal-oxidized SiO_2 layer. Heavily p-doped silicon substrate was employed as a bottom gate electrode. Monolayer graphene was identified by the optical microscope and Raman spectroscopy. The single Lorenz 2D peak (~2700 cm^{-1}), $I_{2D}/I_G>2$ and absence of D peak (~1350 cm^{-1}) demonstrated the quality of the single layer graphene.

EBL Process: Monolayer graphene sheet with lateral sizes of ~4 μm was contacted with Ti/Au (20/80 nm) metal electrodes fabricated by e-beam evaporation after photolithography. Consequently, the graphene channel was patterned into nanoribbons by EBL process. As shown in Figure 1(a)-(d), the electron beam lithography (EBL) can be briefly described as follows. First, hydrogen silsesquioxane (HSQ) was spin-coated on the whole wafer, and the thickness was ~30 nm by using the spin speed of 5000 rpm. Second, the HSQ covered sample was exposed by electron beam with a designed nanoribbon pattern. Third, the exposed sample was developed by NaOH/NaCl salty solution, and the un-exposed HSQ was washed away. Next, the sample was put in the RIE chamber and etched by O_2 plasma, the graphene area with HSQ covering was retained while the other uncovered grahenene parts will be etched away by the O_2 plasma. Last, HSQ resist was washed away by immersing in HF solution (~2%) for 30 seconds.

ALD Process: Hafnia coating was deposited by atomic layer deposition (ALD) (Cambridge Nanotech), the chamber was kept at 50°C before graphene samples were placed inside, and then increased to 270 °C at low vaccum level (10^{-3} mTorr). One single cycle of an ALD is composed of 1-second pulse of TEMAH (tetrakis (ethylmethylamido) hefnium) and successive 1-second pulse of water vapor followed by nitrogen purge of 5 seconds. Different thicknesses of hafnia, 1.8 nm, 3.7 nm, 6.2 nm and 7.8 nm were controlled by using 20, 40, 60 and 80 cycles. The thickness and surface roughness were measured by AFM (Bruker

Dimensiion FastScan, contact mode). The quality of the ALD film was characterized by X-ray Photoelectron spectroscopy (XPS, ESCALAB 250 Xi).

Electrical and Photoresponse Measurements: Electrical characteristics were conducted by a semiconductor device anlyser (Agilent B1500A). Photoresponsivity measurement was performed in a digital deep level transient spectroscopy (DLTS, BIORAD) combined with a four-probe stations. Three light sources (visible: 632 nm semiconductor laser; near infrared: 1470 nm fiber laser; mid-infrared: tunable quantum cascade laser (QCL) from 9.75 μm to 10.48 μm) were employed to illuminate the whole device. The lasers were aligned by optical lens and the power densities of the lasers were assumed to be uniform. All the measurements were conducted at room temperature.

2. Characterization results

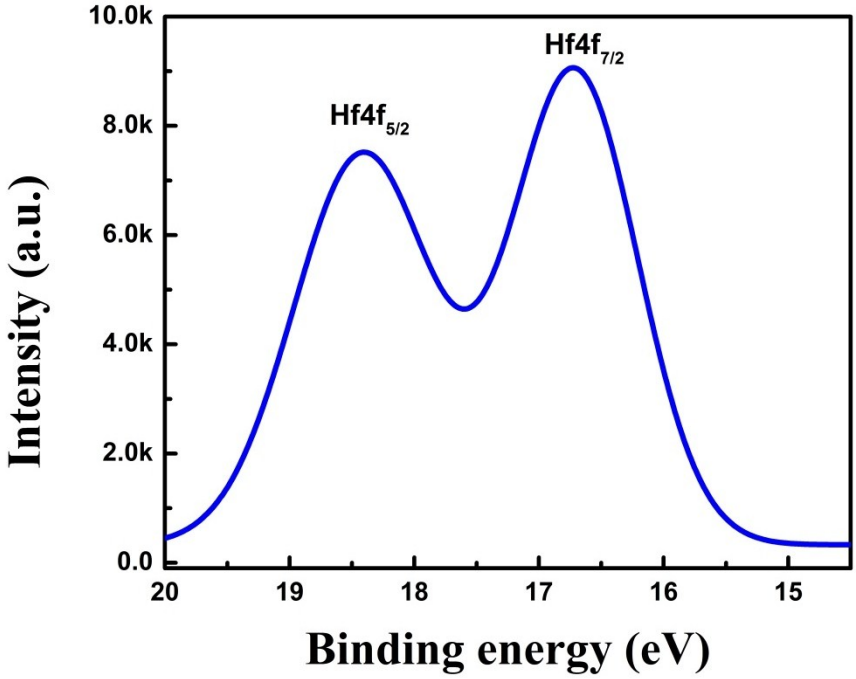

Figure S1. XPS spectra (Hf4f) of the ALD HfO_2 film. The intensity ratio of the Hf 4f 7/2 and Hf 4f 5/2 peaks are constrained to 4:3. The distance of the two peaks is D = 1.71 eV. The Hf 4f 7/2 binding energy for the metal is found at 16.6 eV and is fit with an asymmetric peak-shape. The Hf 4f 7/2 binding energy for the oxide is found ~18.3 eV.

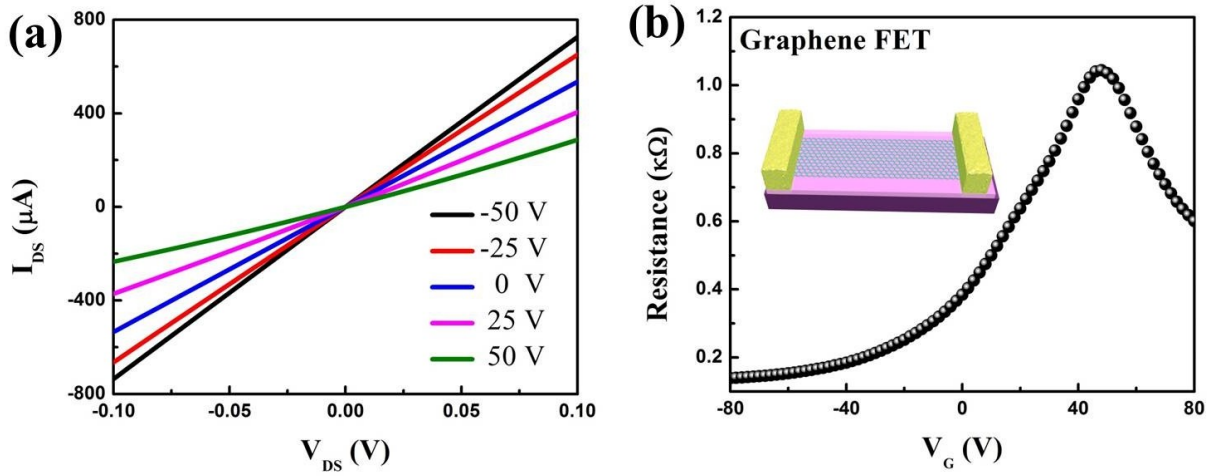

Figure S2. (a) I_{DS}-V_{DS} curves of graphene FET recorded at different gate voltages. (b) Dependenceof graphene FET on gate voltage recorded at V_{DS}=10 mV, indicating a semiconducting behavior curve.

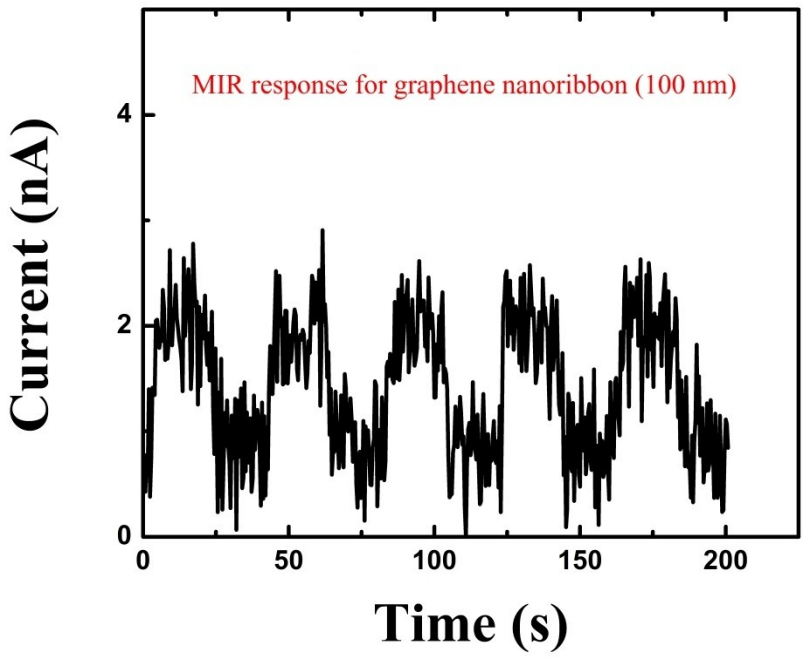

Figure S3. Photoresponse of graphene nanoribbon FET photodetector with a nanoribbon width of 100 nm under a 10 μm laser illumination at room temperature.

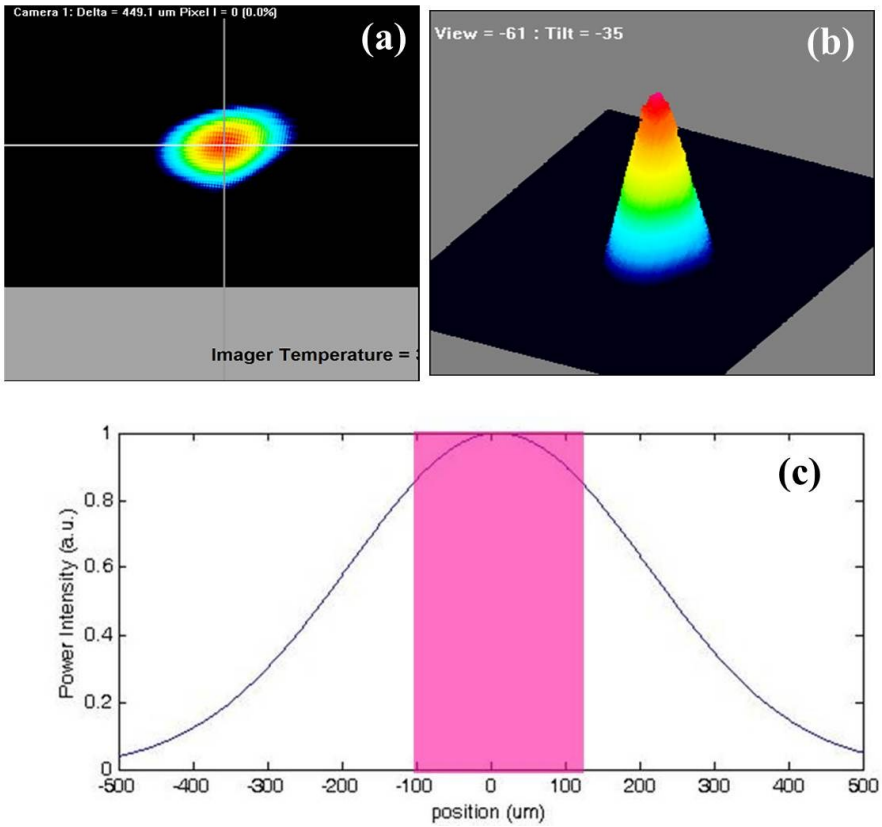

Figure S4. Beam profile of the mid-infrared laser used in our experiment.

3. Calculation of photoresponsivity, gain and detectivity

The photoresponsivity (R) are calculated as the ratio of photocurrent over the optical power on graphene:

$$R = I_{pc} / (P \times 2.3\%)$$

For example, the photon responsivity for this device operated in the visible can be calculated as R = 300 nA/(2.5 W/cm^2 x 4 um x 16 um x 10%) = ~1.75 A/W. Using the same method, we can calculate the photoresponsivity of the near infrared (1.47 μm) and mid-infrared (10 μm) as 1.5 A/W and 0.18 A/W, respectively. The gain and detectivity are calculated as following:

$$G = \frac{I_{ph} / e}{(\frac{S_G}{S_L} \cdot P \cdot 2.3\%) / h\nu} \quad (\nu = \frac{c}{\lambda_{incident}}) \quad \text{and} \quad D = \frac{I_{ph}}{P\sqrt{2eI_{dark}}},$$

where I_{ph} and I_{dark} are the photocurrent dark current, S_G and S_L are the area of the graphene FET channel and light spot, P is the illumination power, υ and λ are the frequency and wavelength of the incident light, e is the electron charge, h is the Planck constant, and c is the speed of light.

4. Calculation of photoconductive gain

The numbers of the photogenerated electrons can be assumed as the consequence of excitation to the conduction band, relaxation from the conduction band, and recombination with holes in the valance band or defects. Thus, we have[S1-S2]

$$\frac{dn_1}{dt} = \chi\beta - Rn_1 - \beta n_1 = 0 \qquad (1)$$

$$\frac{dn_2}{dt} = \alpha n_1 - \frac{n_2}{\tau} = 0 \qquad (2)$$

$$n_1 + n_2 = \frac{I}{e}\tau_t, \qquad (3)$$

where e is the electron charge, n_1 and n_2 are the electron populations in the conduction band and the valance band, R is the recombination rate, I is the measured current, α is the capture rate of electrons, β is the electron generated rate, χ is the multipul excitation factor, τ and τ_t are the measured decay time and transient time. From equations (1) to (3), the capture rate can be expressed by

$$\alpha = \left(\frac{I}{e\chi\beta}\tau_t R - 1\right) \Big/ \left(\tau_1 - \frac{I}{e\chi\beta}\tau\right) \approx \frac{I}{e\chi\beta}\tau_t R/\tau,$$

and the quantum efficiency of carrier multiplication can be expressed by

$$\eta = \frac{\alpha n_1}{\beta} = \frac{\alpha}{\chi(\alpha + \mathrm{R})} \approx \frac{I}{e\chi\beta\tau}\tau.$$

References

[S1] Zhang, Y., Liu, T., Meng, B., Li, X., Liang, G., Hu, X., Wang, Q. J. Nat. Commun. 2013, 4, 1811.

[S2] Winzer, T.; Knorr, A.; Malic, E., Carrier Multiplication in Graphene. *Nano Lett.* **2010**, *10*, 4839.